7. H. Ashkenas and F. S. Sherman, "The structure and utilization of supersonic free jets in low-density wind tunnels," in: Rarefied Gas Dynamics: Fourth Int. Symp., Vol. 2, Academic Press, New York (1966).
8. A. E. Belikov, N. V. Karelov, et al., "Measurements using electron beams. Role of secondary processes in exciting the $B^2\Sigma$ state of the nitrogen ion," in: S. S. Kutateladze and A. K. Rebrova (editors), Diagnostics of Rarefied Gas Glows [in Russian], Inst. Tekh. Fiz. Sib. Otd. Akad. Nauk SSSR, Novosibirsk (1979).
9. A. E. Zarvin and R. G. Sharafutdinov, "Molecular beam generator for studying rarefied gas flows," in: S. S. Kutateladze (editor), Rarefield Gas Dynamics [in Russian], Inst. Tekh. Fiz. Sib. Otd. Akad. Nauk SSSR, Novosibirsk (1976).
10. P. V. Marrone, "Temperature and density measurements in free jets and shock waves," Phys. Fluids, 10, No. 3 (1967).
11. G. Golomb, D. E. Good, et al., "Dimers, clusters, and condensation in free jets. II," J. Chem. Phys., 57, No. 9 (1972).
12. P. A. Skovorodko, "Rotational relaxation with expansion of a gas into a vacuum," in: S. S. Kutateladze (editor), Rarefied Gas Dynamics [in Russian], Inst. Tekh. Fiz. Sib. Otd. Akad. Nauk SSSR, Novosibirsk (1976).
13. R. Cattolica, F. Robben, et al., "Translational nonequilibrium in free jet expansions," Phys. Fluids, 17, No. 10 (1974).
14. G. A. Bird, "Breakdown of translational and rotational equilibrium in gaseous expansions," AIAA J., 8, No. 11 (1970).
15. J. O. Hirshfelder, C. Curtiss, and R. Bird, Molecular Theory of Gases and Liquids, Wiley-Interscience (1964).
16. P. A. Skovorodko and R. G. Sharafutdinov, "Kinetics of population densities of rotational levels in free nitrogen jets," Zh. Prikl. Mekh. Tekh. Fiz., No. 5 (1981).

EXPERIMENTAL INVESTIGATION OF THE CHARACTERISTICS OF SUPERSONIC EXPANSION OF ELECTRIC-ARC PLASMA JETS

G. A. Luk'yanov, V. V. Nazarov, and V. V. Sakhin

UDC 533.9.082.76

Under certain conditions, large deviations from thermodynamic equilibrium are possible with supersonic stationary plasma flow out of a high-pressure chamber into a low-pressure region. Theoretical studies of free supersonic plasma expansion [1-3] and experimental studies of supersonic underexpanded plasma jets [4-6] show that ionization and thermal equilibrium break down in the flow field at some stage of expansion. In this case, the degree of ionization exceeds the equilibrium value, while the electron temperature turns out to be higher than the temperature of heavy particles (atoms and ions). The deviation from equilibrium increases downstream.

The parameters of the plasma in a supersonic jet are closely related to the type of plasma source and flow conditions. In this paper, we attempt to establish the basic parameters that characterize the deviation from ionization and thermal equilibrium and to obtain generalizing dependences for the electron temperature T_e and concentration n_e in the region of free expansion for an argon electric-arc plasma flowing out of a sonic nozzle into a flooded low-pressure region.

1. Conditions and Range of the Investigations. The construction of the plasma source and the scheme of the initial region of the jet are shown in Fig. 1a. The electric-arc source consists of a cathode unit 1 with a tungsten cathode, housing 2, and an anode nozzle 3. We used cylindrical nozzles with diameters d = 2 and 5 mm and length d. The working gas was introduced through tangential openings in the housing. The source was placed inside a vacuum chamber with a volume of 10 m^3 on a coordinated setup with two degrees of freedom in the horizontal plane. The measuring instruments were stationary relative to the vacuum chamber.

Leningrad. Translated from Zhurnal Prikladnoi Mekhaniki i Tekhnicheskoi Fiziki, No. 6, pp. 17-22, November-December, 1981. Original article submitted February 26, 1980.

 0021-8944/81/2206-0744$07.50

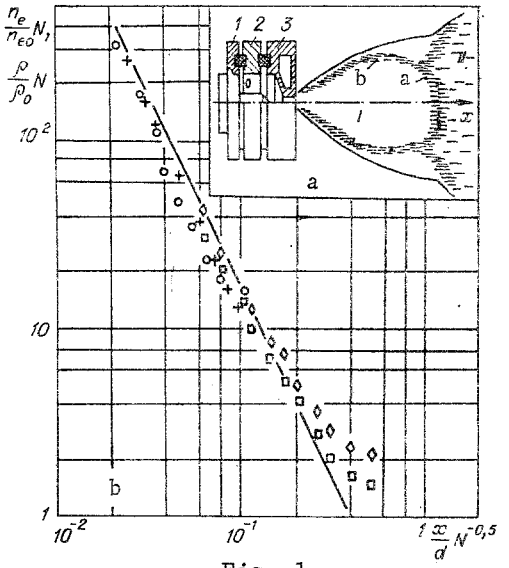

Fig. 1

We performed the experiments in a range of plasma stagnation pressures $p_0 = (1\text{-}8)\cdot 10^4$ Pa and mean mass stagnation temperatures $T_0 = (9.5\text{-}13)\cdot 10^3$ °K. The indicated ranges of p_0 and T_0 correspond to a variation of the arc current strength from 200 to 500 A with the flow rate changing from 0.1 to 0.3 g/sec. The pressure in the vacuum chamber p_∞ varied from 0.4 to 1.3 Pa. The conditions of flow corresponded to degrees of expansion $N = p_0/p_\infty$ from 10^4 to $2\cdot 10^5$. According to the degree of rarefaction, the flow at the initial segment corresponded to a developed transition regime.

The following parameters can be used to characterize the degree of deviation from ionization and thermal equilibrium at the outlet from the source nozzle:

$$K_r = \tau_r/\tau_g, \quad K_h = \tau_h/\tau_g,$$

where τ_r, τ_h, τ_g are the characteristic times of recombination, exchange of energy between electrons and heavy particles, and change in the gasdynamic parameters, respectively.

Assuming that the collisional–radiative recombination and electron–ion energy exchange with elastic collisions play a dominant role, which is valid under the conditions being examined, for τ_r and τ_h we used the following expression [7, 8]:

$$\tau_r = 1/\beta n_e, \quad \beta = 1.75\cdot 10^{-8} n_e T_e^{-9/2}, \quad \tau_h = 250 A T_e^{3/2}/n_e \ln \Lambda,$$

where β is the coefficient of collisional–radiative recombination; A is the atomic weight; and $\ln \Lambda$ is the Coulomb logarithm.

Taking into account the relatively small differences between n_e and T_e at the nozzle cutoff and their values in the arc chamber, on the one hand, and the considerable difficulty in calculating these parameters at the outlet of the nozzle due to the nonisentropic flow along the nozzle, the presence of large transverse gradients, initial thermal and ionization nonequilibrium, on the other hand, it is reasonable to estimate τ_r and τ according to the values of n_e and T_e in the arc chamber, assuming thermodynamic equilibrium for known p_0 and T_0. Equilibrium values of the electron concentrations in the arc chamber n_{e0} for the operational regimes of the source studied are presented in Table 1.

For the characteristic gasdynamic time at the nozzle cutoff, we use

$$\tau_g = \frac{d}{2U_*}, \quad U_* = \left(\gamma \frac{k}{m} T_*\right)^{0.5} \simeq \left(\frac{k}{m} T_0\right)^{0.5},$$

where U_* is the velocity of the plasma in the critical section of the nozzle; γ is the ratio of specific heat capacities; m is the mass of an atom; k is Boltzmann's constant. The range of the investigations is shown by the data in Table 1. We studied the region of free expansion I (see Fig. 1a), separated under the experimental conditions from the mixing zone II by the thickened central a and suspended b density jumps [4, 5].

TABLE 1

$p_0 \cdot 10^{-4}$, Pa	$T_0 \cdot 10^{-3}$, K	$n_{e_0} \cdot 10^{-16}$, cm^{-3}	$N \cdot 10^{-4}$	K_r	K_h	Points on Figs. 1, 3, and 5
1	9,5	0,6	1	1	0,2	1
1,3	10	1	1	0,5	0,1	2
7	10	3	17	0,15	0,1	3
8	13	9	20	0,05	0,02	4

2. Diagnostic Methods. Electric probe and spectral diagnostic methods were used in the experiment. Electric probe methods were used to measure the electron concentration and temperature, and spectral methods were used to measure the temperature T and velocity U of the heavy plasma component. All measurements were carried out along the symmetry axis of the jet.

For the electric probe measurements, we used an electrostatic probe, made of a tungsten wire with a 0.4-mm diameter and a length of 5 mm, soldered to a quartz tube with a 0.8-mm diameter. The quartz tube was placed into a copper water-cooled housing, which served as a reference electrode. In order to study the plasma parameters near the nozzle cutoff, we used a drifting probe, moving with a velocity of ∿5 m/sec across the jet in the section being studied. The current–voltage characteristic of the probe was constructed by points. Usually, 8-10 values of currents on the probe under different probe potentials relative to the reference electrode were given. The values of the current and the applied voltage on the probe were recorded by an N-115 oscillograph. The voltage was supplied by a stabilized B1-8 power supply.

In the region of the jet far away from the nozzle cutoff ($x/d \gtrsim 5$), we used a stationary electrostatic probe, fixed to a stationary water-cooled terminal. A sawtooth voltage from a special mechanical resistance generator with an internal resistance of 3 Ω was applied to the probe. The current–voltage characteristic was recorded by a PDP-4 automatic plotter. The procedure for making electric probe measurements is described in greater detail in [5].

For the spectral measurements, we used an ISP-51 spectrograph with an f = 270 camera or a UF-89 camera and an IT-51-30 Fabry–Perot interferometer. The external setup of the interferometer was used in the parallel beam. The spectra were recorded photographically on Izopankhrom-17 or Izopankhrom-15-1000 film. The spectra were analyzed using heterochromic photometry and an MF-2 microphotometer, whose photocell was replaced by an FÉU-55 photomultiplier. Two methods were used to analyze the spectra: taking into account the fact that the dispersion of the etalon is not constant within a single order when using central rings and measuring in fractions of an order when using single-sided rings.

For measurements of underexpanded plasma jet parameters from the contours of spectral lines, it is necessary to take into account the strong distortion of the contour by the Doppler shift, related to the presence of a radial velocity component. In the experiments carried out, the temperature of the heavy component was measured from the transformation of spectral line contours [9] by comparing the contour of an argon line (main gas) and the contour of a helium line (small admixture up to 5% by volume) under the assumption that there is no relative slippage and that the main gas and the impurity are in thermodynamic equilibrium. The contour transformation method [9] permits determining the temperature, neglecting the instrumental contour of the interferometer and assuming that the true shape of the contours is known. In the measurements carried out, it was assumed that such a transformation permits excluding the instrumental contour and the "expansion" contour from the analysis. The contour transformation procedure was carried out on a computer. The contours of the 0.404-μm ArI and 0.388-μm HeI lines were compared, for which the Stark broadening is negligibly small compared to the Doppler broadening under the experimental conditions. Stark broadening was taken into account with the use of tables from [10] and values of n_e measured by the probe method.

The plasma velocities in the jet were measured according to the Doppler shift of the spectral lines by photographing the spectra head on by rotating the prism system of the spectrograph. The velocities were corrected for the nonuniformity of the distribution of radiation intensity in the jet and the presence of a radial velocity component.

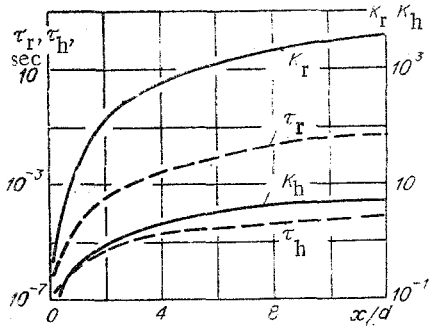

Fig. 2

The spectral measurements were also used to determine the electron concentration from the Stark broadening of spectral lines near the nozzle cutoff, where the flow past the probe differs from a free molecular flow. The data from the probe measurements agreed well with the results determined from broadening of the H_β hydrogen line and from the Stark broadening of different helium lines. The contribution of Doppler broadening to the contour of the observed lines was taken into account using the half-widths of the Voigt contours [11]. The admixture of hydrogen or helium in the argon plasma jet did not exceed 5% by volume of the flow rate of the principal gas.

3. Experimental Results and Their Analysis. Figure 1b shows the results of probe measurements of n_e along the jet axis x in relative coordinates $n_d N/n_{e0}$, $x/dN^{0.5}$. The longitudinal coordinate $x/dN^{0.5} \simeq 0.7$ corresponds to the position of the central density jump for the continuous flow regime. Under the experimental conditions, the extent of the free expansion region along the axis decreases compared to similar flow in a continuous regime due to spreading of the central density jump upwards along the flow [4, 5]. For comparison, Fig. 1b shows the distribution of the relative density of a freely expanding ideal monatomic gas $\rho N/\rho_0$ along the jet axis (continuous line). The similar behavior of the relative densities of the electron component and the gas indicates, first of all, the fact that the composition of the plasma is largely "frozen" in all experiments. An interesting experimental fact is the closeness of the absolute values of the relative densities in the parameter range studied. In the flow field beyond the nozzle cutoff, the degree of ionization is "frozen" and equal to the degree of ionization in the arc chamber, determined assuming thermodynamic equilibrium with respect to the known values of p_0 and T_0. It should be kept in mind that the actual value of the degree of ionization in the arc chamber, due to the initial nonisothermal state, is somewhat higher than the equilibrium value, determined from the mean mass temperature T_0. With flow along the nozzle, the degree of ionization drops. The observed approximate equality of $n_e/n_{e0}N$ and $\rho/\rho_0 N$ is a result of compensation of the factors indicated under the experimental conditions. For $x/d \gtrsim 5$, the experimental data on n_e are approximately described by the dependence

$$\frac{n_e}{n_{e0}} = 0.15\left(\frac{x}{d}\right)^{-2}. \qquad (3.1)$$

Generally speaking, for small K_r some quasiequilibrium region with a considerable drop in the degree of ionization could be expected to remain beyond the nozzle cutoff. However, this was not observed in the experiments. Due to the very intense expansion of the plasma, there is a sharp increase in τ_r and K_r and a breakdown of equilibrium immediately beyond the nozzle cutoff. The distribution of τ_r, K_r, τ_h, and K_h along the jet axis (regime 2, see Table 1) is shown in Fig. 2. The values of τ_r and τ_h were calculated using the experimental values of n_e and T_e. The local gasdynamic characteristic time was determined from the equation $\tau_g = x/U$, where the quantity U was calculated according to the model of an ideal perfect gas with $\gamma = 1.67$. Figure 3 presents the results of measurements of the velocity U on the axis of an argon plasma jet (regime 2). For comparison, the same figure shows the axial distribution of the velocity of a monatomic ideal gas (curve 1) and the value of the maximum velocity for equilibrium flow U_m, calculated from the known magnitude of the mean mass stagnation enthalpy of the plasma $U_m = \sqrt{2H_0}$ (line 2). These curves can be viewed approximately as upper and lower limits for the velocity on the jet axis. The experimental values of the velocity turned out to fall within the range indicated and were near the values for the maximum "frozen" plasma velocity, which agrees with the data presented above on the ionization nonequilibrium.

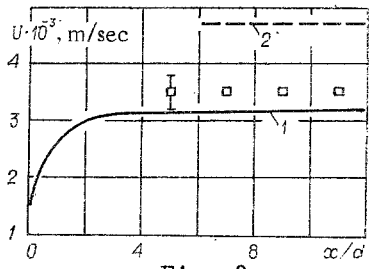

Fig. 3

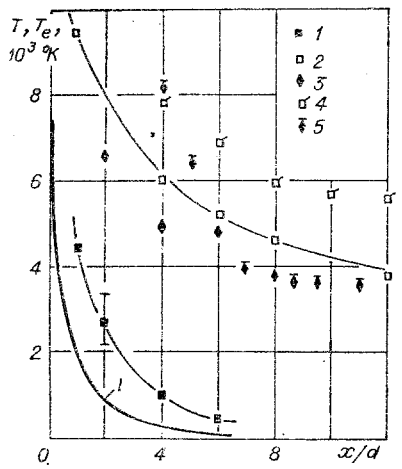

Fig. 4

The results of measurements of T and T_e (points 1 and 2, respectively) are presented in Fig. 4 (regime 2). The experimental values of T are higher by a factor of two to three than the values of T on the axis of a jet of a monatomic ideal perfect gas (curve I). The electronic temperature at x/d = 1 already is twice the temperature T. The ratio T_e/T drops rapidly downstream.

The thermal nonequilibrium situation under similar conditions has not been very well studied experimentally. The results obtained can be compared only to the results in [6], wherein a similar argon plasma jet, generated by a source with nearly the same stagnation parameters, was studied. The experimental data on T from [6] (points 5 in Fig. 4) were obtained, apparently, without taking into account the effect of plasma expansion on the spectral line contours and differ strongly from our results. Figure 4 also presents the values of T (points 3) that we measured without taking into account the radial expansion of the plasma. The values of T obtained in this manner are close to the results in [6]. The nature of the variation in and the magnitude of T_e (points 4), obtained in [6], agree with our results.

For values $K_h \ll 1$ (see Fig. 2), it could have been expected that thermodynamic equilibrium would be approximately satisfied, at least, in some region beyond the nozzle cutoff. However, experiment indicates that thermodynamic equilibrium breaks down practically from the nozzle cutoff. This is explained by the fact that under the experimental conditions with strong breakdown of ionization equilibrium beyond the nozzle cutoff ($K_r > 1$) the electron temperature in the flow field is approximately determined by the energy balance [1, 2]

$$Q^h = Q^r, \quad Q^h = \frac{n_e^2 e^4}{m}\left(\frac{8\pi m_e}{kT_e}\right)^{0.5}\left(1-\frac{T}{T_e}\right)\ln\Lambda, \qquad (3.2)$$

$$Q^r = \left(I^* + \frac{5}{2}kT_e\right)\beta n_e^2,$$

where Q^h is the energy lost by electrons in elastic collisions with ions (collisions with atoms for a degree of ionization $>10^{-4}$ are not important); Q^r is the energy transferred to the electrons during recombination; m_e is the electron mass; I^* is the effective recombina-

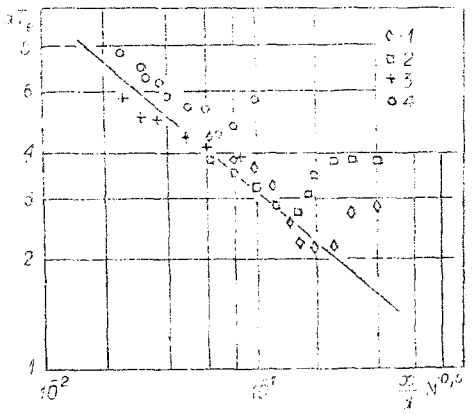

Fig. 5

tion energy. The quantity I* depends on the optical thickness of the plasma. In an optically thick plasma, I* equals the ionization potential I.

For $K_r > 1$, when (3.2) is realized, the condition for thermal equilibrium is written in the form

$$K_h^0 = \frac{\tau_h}{\tau_r}\frac{I^*}{kT_e} = \frac{K_h}{K_r}\frac{I^*}{kT_e} \ll 1. \tag{3.3}$$

Under the experimental conditions, $K_h^0 \gg K_h$. For regime 2, at the nozzle cutoff, $K_h^0 \simeq 3$ with $K_h = 0.1$. The condition for thermal equilibrium $K_h \ll 1$, valid for $K_r < 1$, must be replaced by $K_h^0 \ll 1$ for $K_r \gtrsim 1$.

Let us transform expression (3.2) into the form

$$T_e^4\left(1 - \frac{T}{T_e}\right) = cn_e, \quad c = \frac{1.75\cdot 10^{-8} m\left(I^* + \frac{5}{2}kT_e\right)}{e^4\left(\frac{8\pi m_e}{k}\right)^{0.5}\ln\Lambda}. \tag{3.4}$$

Taking into account (3.1) with $T/T_e \ll 1$, expression (3.4) can be written in the form

$$aT_e = \left(\frac{x}{d}N^{-0.5}\right)^{-0.5}, \quad a = \left(\frac{N}{0.15cn_{e0}}\right)^{0.25}. \tag{3.5}$$

Figure 5 shows a generalization of the experimental data on T_e along the axis of the jet in coordinates aT_e and $x/dN^{0.5}$. The line corresponds to the expression (3.5). The satisfactory generalization and agreement with the approximate theoretical dependence can be seen. As the central density jump is approached, T_e increases and relation (3.5) breaks down.

Thus, for $K_r > 0.05$ and $K_h > 0.02$ (at the nozzle cutoff), it is possible to generalize the axial profiles of the relative electron concentrations and temperatures in the free expansion region of the argon plasma jets studied.

LITERATURE CITED

1. G. A. Luk'yanov, "Stationary supersonic equilibrium plasma source," Zh. Prikl. Mekh. Tekh. Fiz., No. 6 (1968).
2. D. A. Bartenev and G. A. Luk'yanov, "Calculation of axisymmetrical free expansion of a nonequilibrium hydrogen plasma," Zh. Prikl. Mekh. Tekh. Fiz., No. 4 (1972).
3. Y. S. Chou and L. Talbot, "Source-flow expansion of a partially ionized gas into a vacuum," AIAA J., 5, No. 12 (1967).
4. G. A. Luk'yanov, "Relaxation of electron temperature and concentration in a supersonic rarefied plasma jet," in: Problems in the Physics of Low-Temperature Plasma, Nauka i Tekhnika, Minsk (1970).
5. G. A. Luk'yanov and G. V. Petukhov, "Probe measurements in a rarefied plasma jet," Teplofiz. Vys. Temp., 7, No. 5 (1969).
6. T. Yoshikawa and T. Murasaki, "Heavy-particle velocity and temperature measurement in a supersonic arc-heated plasma flow," AIAA Paper No. 75-862 (1975).

7. A. V. Gurevich and L. P. Pitaevskii, "Recombination coefficient in a dense low-temperature plasma," Zh. Eksp. Teor. Fiz., 46, No. 4 (1964).
8. Ya. B. Zel'dovich and Yu. P. Raizer, Physics of Shock Waves and High-Temperature Hydrodynamic Phenomena [in Russian], Nauka, Moscow (1966).
9. M. P. Chaika and É. E. Fradkin, "Method for transforming spectral line contours and its application to measuring the temperature and other parameters of a light source," Opt. Spektrosk., 7, No. 9 (1959).
10. H. R. Griem, Plasma Spectroscopy, McGraw-Hill, New York (1964).
11. V. Vize, "Width of spectral lines," in: Plasma Diagnostics [Russian translation], Mir, Moscow (1967).

EXPERIMENTAL INVESTIGATION OF INTERACTION OF A SHOCK WAVE WITH A WALL CAVITY

E. F. Zhigalko, L. L. Kolyshkina, and V. D. Shevtsov

UDC 533.601.1

In unsteady gas flow one often meets the situation where a shock wave passes a location where the channel section changes. At a very early stage of the phenomenon, when there is no appreciable interference by structural elements, it is profitable to examine the phenomenon as a combination of elementary characteristic model problems in shock-wave–wall interaction. At a later stage it is often possible to use a one-dimensional approach and employ solutions of the discontinuity decay problem [1-3]. The investigation of the intermediate stage in this paper is based on experiments conducted in an air shock tube of rectangular section 130 × 80 mm whose channel overlaps a rigid wall normal to the tube axis, with a straight cavity of finite length. The examination concentrates on questions not inherently associated with the finite nature of the channel section ahead of the model.

The unsteady process examined here can be arbitrarily divided into phases, in accordance, for example, with changes in the wave configurations in each phase.

While the incident wave is penetrating the cavity, the gas, compressed behind the shock wave reflected from the forward sections of the wall, is flowing into the cavity, where the pressure is lower. The diffracted waves from the opposite edges repeatedly interact with each other and with the obstacle, thus modulating both the reflected wave and the wave penetrating the cavity.

Until one has a wave going through the channel its base pressure has the property of similarity for channels of different width H. The similarity does not extend to elements of the phenomenon which are intrinsically connected with the influence of dissipation, e.g., to the separation accompanying gas flow over the forward edges of the cavity. The sequence of vortices formed here is carried by the flow into the cavity, generating two systems of vortices about its walls, like Kármán streets, clearly visible on shadowgraph and interferometry pictures (Fig. 1a).

With the onset of the next phase when the wave in the cavity reaches the floor and reflects from it, the channel length L is added to the parameters of the problem. In modeling this and subsequent phases one can use only results consonant with similarity of flows about cavities of the same L/H ratio. One can consider, arbitrarily, that the second phase lasts until the shock wave reflected from the floor exits from the channel and the rarefaction wave penetrates into it.

Figure 2 (H = 10 mm) shows typical oscillograms obtained in calibrating a piezometric pressure sensor in a shock tube with the end closed (Fig. 2a, M = 1, 2), and in measurement of the pressure at characteristic points on the model: on the floor (Fig. 2b, M = 1.44) and at the forward edge (Fig. 2c, M = 1.24). Some of the sensor parameters are: sensitive element diameter 1.5 mm, maximum body diameter 6 mm, estimated self-frequency no lower than 100 kHz.

Leningrad. Translated from Zhurnal Prikladnoi Mekhaniki i Tekhnicheskoi Fiziki, No. 6, pp. 23-28, November-December, 1981. Original article submitted March 17, 1980.

 0021-8944/81/2206-0750$07.50